Investigation of Groundwater Flow Using $\Delta^{18}O$ and ΔD in a Sulfur Mine in Japan

Shinji MATSUMOTO[1], Isao MACHIDA[2]

[1] National Institute of Advanced Industrial Science and Technology, Geological Survey of Japan, Geo-Resources and Environment, Groundwater Research Group Central 7, 1-1-1, Higashi, Tsukuba, Ibaraki, Japan; email: shin.matsumoto@aist.go.jp
[2] National Institute of Advanced Industrial Science and Technology, Geological Survey of Japan, Geo-Resources and Environment, Groundwater Research Group Central 7, 1-1-1, Higashi, Tsukuba, Ibaraki, Japan; email: i-machida@aist.go.jp

Abstract

The A sulfur mine is located in the Iwate Prefecture of Japan. This mine has both surface and underground parts and was operated from the late 1800s to the late 1900s. Since the early 1900s, acid mine drainage (AMD) has been reported in this mine, and the waste water has been neutralized in a treatment plant since the mine was closed. Recently, reducing the AMD volume by decreasing water inflow to the underground mine has been considered as a way to reduce the AMD treatment cost. The first step in such an approach is to understand in detail the groundwater flow around the mine. However, part of the study area is covered by lava and comprises crystalline rocks with complicated structures, making it difficult to understand the groundwater flow. Therefore, the present study investigated the groundwater flow around this mine by focusing on water quality, such as pH and electrical conductivity (EC), stable isotopes (i.e. δ18O and δD) and 3H in the surface and ground water. The spatial distributions of pH, Stiff diagrams, and δ18O and δD values in the surface and ground water indicated that the groundwater flow system was divided into three basins in the study area, as predicted from geomorphological information. Moreover, the spatial distribution of δ18O and δD in the surface and ground water suggested that the groundwater recharged at the highest altitudes in the B mountain in the northwest of the mine might flow in the underground mine. Furthermore, the 3H values in the waste water discharged from the underground part of mine implied that the groundwater age was no more than approximately 60 years old.

Keywords: *mine closure, acid mine drainage (AMD), waste water, stable isotopes, groundwater flow*

Introduction

The A sulfur mine is located in the Iwate Prefecture of Japan. This mine has both surface and underground parts. This mine began operation in the late 1800s but was closed in the late 1900s because of falling demand for sulfur. Since the early 1900s, the serious water-pollution problem of acid mine drainage (AMD) has been reported in this mine, and the waste water discharged from the underground mine has been neutralized in a treatment plant since the mine closed. However, treating this AMD is very expensive and voluminous (e.g., approximately 9.1 million cubic meters of AMD with a pH of 2.3 were treated in 2006). Reducing the AMD volume by decreasing water inflow to the underground mine has been considered as a way to reduce the AMD treatment cost. The first step in such an approach is to understand the groundwater flow around the mine. A reliable method for understanding groundwater flow is to use information about the stable isotopes of water, such as $\delta^{18}O$ and δD. The isotope tracer technique began in the 1950s in the field of hydrology, and by the late 1960s isotopes were being used widely in hydrology research worldwide (Huang and Wang, 2017). In recent years, the composition of stable water isotopes has been used effectively to investigate groundwater flow around mine sites. Gammons et al. (2010) used $\delta^{18}O$ and δD to understand the recharge area of inflow into abandoned coal mines, and Toughzaoui et al. (2015) used $\delta^{18}O$ and δD isotope analysis to investigate hydrological processes around an abandoned mine watershed. Huang and Wang (2017) showed several examples

of using $\delta^{18}O$ and δD as mine groundwater tracers, and they used the isotopic data of water samples taken from the study area to simulate numerically the groundwater recharge area. Furthermore, the impact of AMD can be discussed based on the $\delta^{18}O$ and δD values of surface water around a mine area (Sun et al., 2014). However, part of the area in the present study is covered by lava and comprises crystalline rocks with complicated structures, making it difficult to understand the groundwater flow. In addition, $\delta^{18}O$ and δD have not been used previously to investigate water inflow to the underground part of this mine. Therefore, the present study investigates the groundwater flow around the A sulfur mine by using geochemical methods, water quality, such as pH and electrical conductivity (EC), stable isotopes (i.e. $\delta^{18}O$ and δD which are used widely as tracers), and ^3H in surface and ground water.

Materials and methods

Figure 1 shows a topographic map of the study area with the locations of (i) the sampling sites (A1–A6, B1–B17, and C1–C8), (ii) the B mountain, and (iii) the underground mine area. Figure 2 provides geological information about the study area (Kawano and Uemura, 1962). The underground mine area is located at approximately 1,000 m above sea level. In Fig. 1, based on the geomorphological information, the groundwater flow system is divided into basins A, B, and C. In Fig. 2, the alteration zones, which are affected by silicidation and argillation, include sulfur deposits (L1 and L2) and are covered with unaltered lava (L3–L5) (Kawano and Uemura,
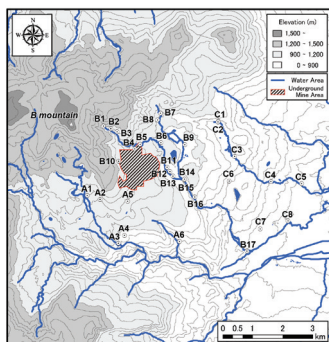
Fig. 1. Topographic map of study area with locations of sampling sites, B mountain, and underground mine area
Rys. 1. Mapa topograficzna obszaru badań z lokalizacjami miejsc pobierania próbek, góry B i obszaru kopalni podziemnej
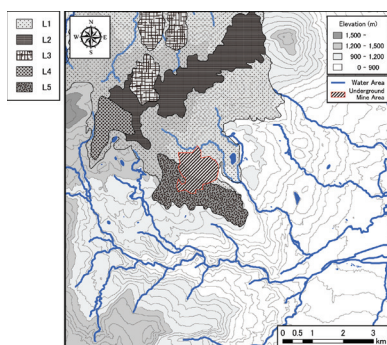

Fig. 2. Geological map of study area: L1 is andesitic tuff with augite-hypersthene andesite lava; L2 is quartz-bearing olivine-augite-hypersthene andesite and augite-hypersthene andesite; L3 is augite-hypersthene-olivine basalt; L4 is augite-olivine-hyperthene andesite; L5 is olivine-augite-hypersthene andesite (Kawano and Uemura, 1962)
Rys. 2. Mapa geologiczna badanego obszaru: L1 jest tufem andezytycznym z lawą andezytową hiperstenem; L2 to zawierający kwarc oliwinowy augit-augit-hipersten andezyt i augit-hipersten andezyt; L3 jest augit-hipersten-oliwin bazaltem; L4 to andezyt-augit-oliwin-hiperten; L5 jest andezytem oliwinu-augitu-hiperstenu (Kawano i Uemura, 1962)
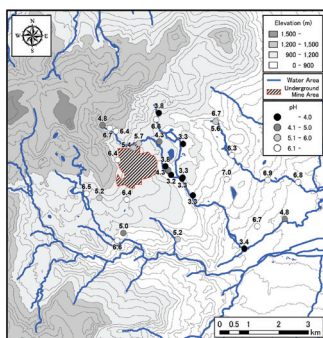

Fig. 3. Spatial distribution of pH of water samples
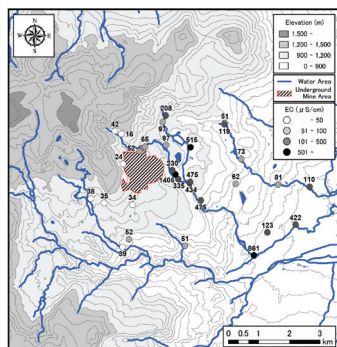Rys. 3. Przestrzenny rozkład pH próbek wody

Fig. 4. Spatial distribution of EC of water samples
Rys. 4. Przestrzenny rozkład EC próbek wody

Tab. 1. Chemical characteristics of surface and ground water in study area
Tab. 1. Charakterystyka chemiczna wód powierzchniowych i gruntowych na badanym obszarze

Samples	Temp (°C)	pH (-)	EC (µS/cm)	Fe^{total} (mg/L)	Na$^+$ (mg/L)	K$^+$ (mg/L)	Ca^{2+} (mg/L)	Mg^{2+} (mg/L)	Cl$^-$ (mg/L)	HCO$_3^-$ (mg/L)	SO$_4^{2-}$ (mg/L)	δ^{18}O (‰)	δD (‰)	^{3}H (T.U.)
A1	5.1	6.5	40	0.1	2.6	0.5	3.1	1.0	3.2	6.5	2.6	−10.4	−66	3.9
A2	5.4	5.2	40	0.0	2.3	0.5	2.0	0.9	3.9	7.7	5.4	−10.2	−63	-
A3	5.3	6.6	40	0.0	2.5	0.5	3.2	1.0	3.4	11.8	2.2	−10.7	−65	-
A4	5.4	5.0	50	0.0	2.9	0.7	3.3	1.3	3.8	2.4	13.3	−10.4	−64	-
A5	5.1	6.4	30	0.0	2.3	0.4	2.9	0.8	2.1	11.8	2.7	−11.8	−74	-
A6	5.0	5.2	50	0.0	2.5	0.6	3.4	1.3	2.7	6.9	13.8	−11.0	−69	3.9
B1	-	4.8	-	0.1	2.3	0.5	3.6	1.4	2.4	0.0	20.3	−11.4	−70	3.8
B2	3.6	6.7	40	0.0	3.0	0.7	3.3	1.2	2.6	4.5	7.4	−11.6	−73	3.5
B3	3.0	6.4	20	0.0	1.5	0.3	1.1	0.5	2.6	6.1	2.3	−10.6	−66	-
B4	5.4	5.4	50	0.1	2.3	0.5	4.4	1.5	2.8	6.9	16.3	−10.8	−67	-
B5	3.4	5.7	70	0.1	2.3	0.5	4.7	1.6	2.5	0.0	21.0	−11.4	−71	-
B6	5.2	4.3	100	0.1	2.3	0.7	5.2	1.4	3.0	0.0	30.5	−10.3	−63	-
B7	5.4	3.8	210	0.1	2.8	0.8	7.1	2.2	2.2	0.0	68.0	−11.2	−69	4.6
B8	5.7	6.6	100	0.0	4.8	0.6	8.9	2.4	2.7	8.5	33.9	−11.8	−74	3.8
B9	7.4	3.3	520	0.3	5.5	2.4	30.0	3.8	3.9	0.0	152.1	−11.1	−69	-
B10	5.4	6.4	20	0.0	1.8	0.3	1.9	0.7	2.0	8.1	5.5	−11.7	−73	-
B11	4.4	3.8	230	0.1	3.1	0.8	9.9	2.8	2.8	0.0	81.2	−11.0	−68	-
B12	13.0	4.3	1410	0.0	8.4	3.2	254.4	8.7	2.6	0.0	877.2	−11.8	−74	-
B13	7.3	3.2	340	0.3	3.2	0.8	6.5	2.1	2.2	0.0	86.3	−11.5	−73	3.8
B14	8.0	3.3	480	0.2	5.5	3.2	30.1	3.8	4.6	0.0	150.3	−11.0	−68	-
B15	7.4	3.3	430	0.4	3.7	1.2	17.3	3.3	3.1	0.0	157.0	−10.4	−63	-
B16	7.5	3.3	480	0.5	4.2	1.7	22.1	3.3	3.4	0.0	160.4	−10.5	−63	-
B17	9.5	3.4	860	0.2	6.7	2.5	109.6	6.3	3.0	0.0	446.8	−11.2	−70	-
C1	7.1	6.7	50	0.0	3.1	1.2	4.3	1.5	2.6	30.5	4.2	−11.8	−75	3.5
C2	8.7	5.6	120	0.0	5.4	1.7	8.1	2.9	4.2	6.5	37.4	−11.3	−71	0.6
C3	5.8	6.3	70	0.1	3.7	1.1	5.6	2.0	3.3	9.4	21.8	−11.4	−72	-
C4	5.2	6.9	80	0.0	3.8	1.1	5.8	2.1	3.2	9.4	22.6	−11.4	−73	-
C5	8.1	6.8	110	0.0	4.6	1.2	10.6	3.1	3.3	15.5	31.9	−11.4	−73	-
C6	7.8	7.0	60	0.0	3.1	0.4	4.8	2.3	4.9	29.7	32.0	−11.5	−74	2.9
C7	7.5	6.7	120	0.0	4.5	1.7	12.0	3.2	4.1	10.6	43.3	−10.6	−68	-
C8	9.7	4.8	420	0.0	10.4	2.9	44.3	9.2	6.4	0.0	205.0	−10.5	−68	3.3
Average	6.4	5.3	220	0.1	3.8	1.1	20.4	2.6	3.2	6.2	87.9	−11.1	−69	3.4

1962). The waste water from the underground mine is neutralized in the treatment plant at B12 in Fig. 1 before being discharged into the river (the pH of the final effluent water is maintained at above 4.0 based on the limits regarding the waste water quality in this mine). There is also a water drain hole at B10 to decrease the volume of recharging water into the underground mine.

Samples of surface and ground water for chemical and isotopic analyses were taken between October 30, 2018 and November 1, 2018 at the 31 sampling sites shown in Fig. 1. During the sampling, the chemical characteristics of the water [i.e., temperature, pH, and EC] were measured in the field using a colorimetric pH measuring device (ATC series; Advantec, Japan), a pH meter (D52S; Horiba, Japan), and an EC meter (YSI-Pro30; YSI, USA). Collected in 100 mL polyethylene bottles, the water samples were analyzed for alkalinity, inorganic ions (Fe^{total}, Na$^+$, K$^+$, Ca^{2+}, Mg^{2+}, Cl$^-$, SO$_4^{2-}$), and stable isotope of water (δ^{18}O and δD) after filtration using disposable 0.45 µm in-line filters. The alkalinity (pH 4.8) was measured using 0.02N H$_2$SO$_4$ titration method, and the result was converted to a concentration of HCO$_3^-$. The concentrations of Fe^{total} and Mg^{2+} were measured using ICP-MS (NexION 300; PerkinElmer, USA) after adding HNO$_3$ to lower the pH to below 2, and those of Na$^+$, K$^+$, Ca^{2+}, Cl$^-$, and SO$_4^{2-}$ were measured using ion chromatography (ICS-5000; Dionex, USA). The δ^{18}O and δD values were determined using a liquid water isotope analyzer (L2140-i; Picarro, USA) employing a cavity ring-down spectrometer with analytical errors within ± 0.1‰ for δ^{18}O and ± 1‰ for δD. The δ^{18}O and δD values were expressed relative to Vienna Standard Mean Ocean Water. Additionally, water samples in 1,000 mL polyethylene bottles were taken at 11 sampling sites for ^{3}H analysis. They were distilled under reduced pressure using an automated evaporator (NVC2200 and N-2100; Eyela, Japan) prior to electrolytic accumulation of ^{3}H by an electrolysis instrument (Tori Pure; Permerec, Japan). The ^{3}H concentrations of the samples were determined using a liquid scintillation counter (AccuFLEX LSC-LB7; Hitachi Aloka, Japan) with an analytical error within ± 0.28 tritium unit (T.U.). The analytical data were plotted using ArcGIS 10.5 (ESRI, USA).

Results and discussion

The quality of the water samples is summarized in Table 1, and Figs. 3 and 4 show the spatial distributions of pH and EC in the study area. The B12 water sample had the highest temperature, EC, and SO$_4^{2-}$. Because the treatment plant for the waste water from the underground mine is at B12, the pH there exceeded 4.0 and was within the regulations for waste water quality in this mine. Although the surface water at A1–A4 showed pH values greater than 5.0 (the average pH was 5.8) and that at C1–C5 showed pH values greater than 5.6 (the average pH was 6.5), a low pH was observed in the surface water around the underground mine area in Fig. 3; the pH values at B9 and B13–B16 were less than 3.3. Given that the pH of the treated water at B12 was 4.3, the low pH around the underground mine area is not due to the waste water from the underground mine. In Fig. 2, the alteration zones (L1) including the sulfur deposit cover the B7, B9, B11, B13, and B14 sampling sites, where the pH of the surface water was less than 4.0. Furthermore, the SO$_4^{2-}$ concentration exceeded 68.0 mg/L (the average value was 107.6 mg/L) and that of Fe^{total} exceeded 0.1 mg/L (the average value was 0.2 mg/L), show-
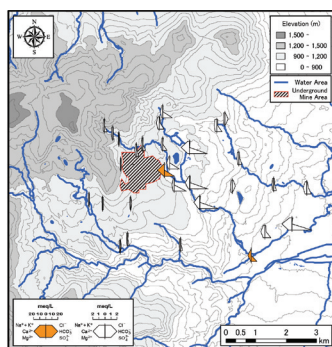
Fig. 5. Stiff diagrams of water samples
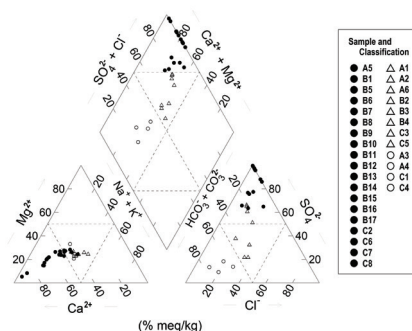Rys. 5. Diagramy Stiffa próbek wody

Fig. 6. Piper diagram of water samples
Rys. 6. Chemizm próbek wody

ing higher values than the overall average values of SO_4^{2-} and Fe^{total} in the study area. This indicates that the acidic water (pH < 4.0) may be due to the exposure of sulfide minerals in the L1 layer in Fig. 2, leading to the pH being less than 3.4 at B9 and B13–B16.

In Table 1, the ^3H values are between 2.9 and 4.6 at all sampling sites except C2. The C2 water sample was collected in wetland with stagnant water areas, causing an ^3H value of 0.6 T.U. According to Kazemi et al. (2006), the concentration of ^3H in rainfall was observed as early as 1953 because of thermonuclear tests around the world; it peaked in 1963 and 1964 and has decreased since then. This suggests that the groundwater ages around the underground mine are less than approximately 60 years old.

Figure 5 shows the spatial distribution of Stiff diagrams, and Fig. 6 shows the Piper diagram based on the water quality in Table 1. The Stiff diagrams with high concentration of SO_4^{2-} and Ca^{2+} were plotted at the middle stream and downstream of the river located east of the underground mine, although the Stiff diagrams were smaller upstream of the river. The Stiff diagrams at A1–A6 were the smallest, followed by those at C1–C7. These results show that the groundwater flow system can be divided into three basins in the study area (A, B, and C), as predicted based on geomorphological information. In Fig. 6, most of the analytical results at B1–B17 as shown in Table 1 were plotted in the Piper diagram with SO_4^{2-} + Cl^- > 60% and Ca^{2+} + Mg^{2+} > 60%. By contrast, surface water with SO_4^{2-} + Cl^- < 50% and Ca^{2+} + Mg^{2+} > 60% was sampled at A3, A4, C1, and C4. Thus, the quality of the surface water and ground water in the study area is characterized by SO_4^{2-}, which is attributed to the generation of AMD.

The spatial distributions of stable isotopes of the water samples ($\delta^{18}O$ and δD) are summarized in Fig. 7 based on the analytical data in Table 1, and the relationship between $\delta^{18}O$ and δD is described in Fig. 8. The respective values of $\delta^{18}O$ and δD were −11.7‰ and −73‰ at B10 and −11.8‰ and −74‰ at A5 and B12, indicating lower $\delta^{18}O$ and δD values than the overall average ones. The values of $\delta^{18}O$ and δD are generally lower in water from higher altitude (known as the altitude effect) (Florea et al., 2017; Clark and Fritz, 1997). Regarding the spatial distributions of $\delta^{18}O$ and δD, the rain water recharged at the B mountain with the highest altitude of approximately 1,600 m in the study area may flow in B10, A5, and B12 through the underground mine area. The values of $\delta^{18}O$ and δD at A1–A4 were $\delta^{18}O \geqq -10.7$‰ and $\delta D \geqq -66$‰, suggesting that the surface water at the sampling sites comes from an area lower than B mountain. By contrast, the average values of $\delta^{18}O$ and δD at C1–5 were −11.5‰ and −73‰, respectively, showing lower values than the overall average ones. Therefore, the surface water at C1–C5 may come from the high-altitude area in the northeast of the study area. Because lava is generally porous and cannot hold water (Leopold et al., 2016), rain water may be supplied to the underground mine area from B mountain through lava described as L3, L4, and L5 in Fig. 2 on the basis of the spatial distributions of $\delta^{18}O$ and δD. In addition, Fig. 8 shows good correlation between $\delta^{18}O$ and δD. The values were plotted between the meteoric water line with "d-excess" values of 10 and 25, and the same trend was observed in a previous study (Suzuki and Tase, 2014).

Consequently, the quality of the surface and ground water in the present study was characterized by SO_4^{2-} from sulfide minerals in the sulfur deposit. The acidic water at the middle
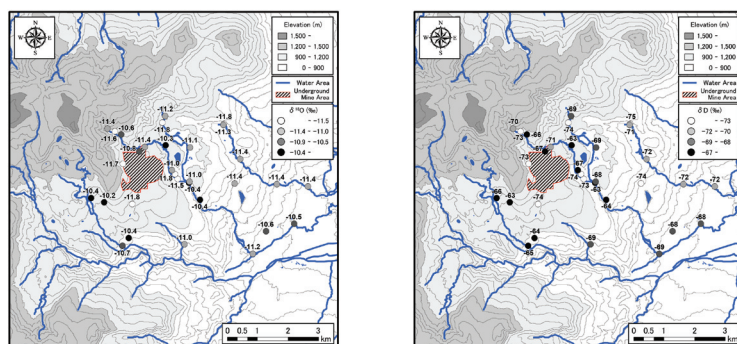
Fig. 7. Spatial distributions of $\delta^{18}O$ (left) and δD (right) in water samples
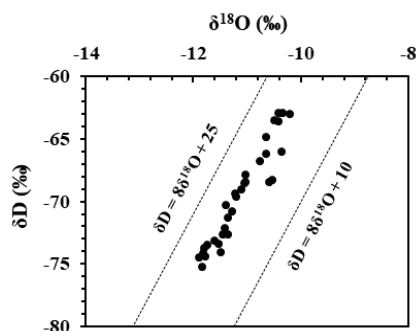Rys. 7. Rozkłady przestrzenne $\delta^{18}O$ (po lewej) i δD (po prawej) w próbkach wody

Fig. 8. Relationship between $\delta^{18}O$ and δD in water samples
Rys. 8. Zależność między $\delta 1^{8O}$ i δD w próbkach wody

and downstream of the river located east of the underground mine is not attributed to waste water from the underground mine. The surface and ground water at A5 and B10 might come from water recharged in the B mountain area based on the spatial distributions of $\delta^{18}O$ and δD, and it flows into B12 through the underground mine area. Although more data are required to determine the area recharging the underground mine area, doing so would help to reduce the AMD volume by decreasing water inflow to the underground mine. Thus, the hydrogeochemical and isotopic data of surface and ground water can provide information that is important for understanding hydrological processes around the mine site and assessing how the mine waste water impacts the surrounding environment.

Conclusions

This research investigates groundwater flow around the A sulfur mine by using geochemical methods, water quality, such as pH and EC, stable isotopes (i.e. $\delta^{18}O$ and δD) and ^3H in surface and ground water. The distributions of pH, Stiff diagrams, and $\delta^{18}O$ and δD in surface and ground water indicated that the groundwater flow system was divided into three basins in the study area, corresponding to the flow system predicted based on geomorphological information. The results also suggested that the quality of the surface and ground water in the study area was characterized by SO_4^{2-} from sulfide minerals in the sulfur deposit. Furthermore, the groundwater recharged at the highest altitudes in the B mountain in the northwest of the underground mine might flow in the underground mine based on the distribution of $\delta^{18}O$ and δD in the surface and ground water. Furthermore, the value of ^3H in the waste water from the underground part of mine implied that the groundwater age was less than approximately 60 years old.

Acknowledgments

Literatura – References

1. CLARK, D. Ian and FRITZ, Peter. Environmental isotopes in hydrogeology. Lewis Publishers: New York, 1997, p. 352.

2. FLOREA, Lee et al. Stable isotopes of river water and groundwater along altitudinal gradients in the high Himalayas and the Eastern Nyainqentanghla mountains. In Journal of Hydrology: Regional Studies, 14, 2017, p.37-48.

3. GAMMONS, H. Christopher et al. Geochemistry and stable isotope investigation of acid mine drainage associated with abandoned coal mines in central Montana, USA. In Chemical Geology, 269(1-2), 2010, p. 100-112.

4. HUANG, Pinghua and WANG, Xinyi. Applying environmental isotope theory to groundwater recharge in the Jiaozuo mining area, China. In Geofluids, 2017(1), 2017, p. 1-11.

5. KAWANO, Yoshinori and UEMURA, Fujio. Explanatory text of the geological map of Japan, Scale 1:50000, Hachimantai. Geological Survey of Japan, 1962.

6. KAZEMI, A. Gholam et al. Groundwater Age. John Wiley & Sons: Hoboken, 2006, p. 346.

7. LEOPOLD, Matthias et al. Subsurface architecture of two tropical alpine desert cinder cones that hold water. In Journal of Geophysical Research: Earth Surface, 121(6), 2016, p. 1148-1160.

8. SUN, Jing et al. Hydrogen and oxygen isotopic composition of karst waters with and without acid mine drainage: impacts at a SW China coalfield. In Science of the Total Environment, 487(15), 2014, p. 123-129.

9. SUZUKI, Hidekazu and TASE, Norio. Origin and geochemistry of a flowing confined groundwater at the northern foot of Mt. Iwate, Northeast Japan. In Komazawa Journal of Geography, 50, 2014, p. 101-111, In Japanese.

10. TOUGHZAOUI, Sana et al. Hydrogeochemical and isotopic studies of the Kettara mine watershed, Morocco. In Mine Water and the Environment, 34(3), 2015, p. 308-319.

Badanie przepływu wód podziemnych za pomocą $\Delta^{18}O$ i ΔD w kopalni siarki w Japonii

Kopalnia siarki znajduje się w prefekturze Iwate w Japonii. Kopalnia ma zarówno części naziemne, jak i podziemne i działała od końca 1800 roku do końca XX wieku. Od początku XX wieku odnotowano w tej kopalni kwaśny drenaż kopalniany (AMD), a ścieki były zneutralizowane w oczyszczalni do czasu zamknięcia kopalni. Ostatnio uznano, że zmniejszenie objętości AMD przez zmniejszenie dopływu wody do podziemnej kopalni jest dobrym sposobem na zmniejszenie kosztów neutralizacji AMD. Pierwszym krokiem w takim podejściu jest szczegółowa analiza przepływu wód gruntowych wokół kopalni. Jednak część obszaru objętego badaniem jest pokryta lawą i obejmuje skały krystaliczne o skomplikowanych strukturach, co utrudnia zrozumienie przepływu wód gruntowych. Dlatego w niniejszych badaniach określono przepływ wód podziemnych wokół tej kopalni, koncentrując się na jakości wody, określono parametry takie jak pH i przewodność elektryczna (EC), stabilne izotopy (tj. $\Delta^{18}O$ i δD) oraz 3H w wodzie powierzchniowej i gruntowej. Przestrzenne rozkłady odczynu pH, wartości $\delta^{18}O$ i δD w wodzie powierzchniowej i gruntowej wskazały, że system przepływu wód podziemnych został podzielony na trzy baseny na badanym obszarze, zgodnie z przewidywaniami z informacji geomorfologicznej. Ponadto rozkład przestrzenny $\delta^{18}O$ i δD w wodach powierzchniowych i gruntowych sugerował, że wody gruntowe dopływające na najwyższych wysokościach w północno-zachodniej części kopalni mogą płynąć do części podziemnej kopalni. Co więcej, wartości 3H w ściekach odprowadzanych z podziemnej części kopalni sugerowały, że wiek wód podziemnych wynosił nie więcej niż około 60 lat.

Słowa kluczowe: zamknięcie kopalni, kwaśny drenaż kopalniany (AMD), ścieki, stabilne izotopy, przepływ wód gruntowych